Vol 17 No 7, July 2008
1674-1056/2008/17(07)/2562-05

Chinese Physics B

© 2008 Chin. Phys. Soc.
and IOP Publishing Ltd

Design, fabrication and characterization of a high-performance microring resonator in silicon-on-insulator*

Huang Qing-Zhong(黄庆忠), Yu Jin-Zhong(余金中)†, Chen Shao-Wu(陈少武), Xu Xue-Jun(徐学俊), Han Wei-Hua(韩伟华), and Fan Zhong-Chao(樊中朝)

National Key Laboratory on Integrated Optoelectronics, Institute of Semiconductors, Chinese Academy of Sciences, Beijing 100083, *China*

(Received 8 November 2007; revised manuscript received 21 December 2007)

A high-performance microring resonator in a silicon-on-insulator rib waveguide is realized by using the electron beam lithography followed by inductively coupled plasma etching. The design and the experimental realization of this device are presented in detail. In addition to improving relevant processes to minimize propagation loss, the coupling efficiency between the ring and the bus is carefully chosen to approach a critical coupling for high performance operating. We have measured a quality factor of 21,200 and an extinction ratio of 12.5dB at a resonant wavelength of 1549.32nm. Meanwhile, a low propagation loss of 0.89dB/mm in a curved waveguide with a bending radius of 40μm is demonstrated as well.

Keywords: integrated photonics, microring resonator, quality factor, silicon-on-insulator
PACC: 4280L, 4282, 4225B

1. Introduction

In recent years, microring resonators have attracted considerable attention, due to their applications in various kinds of integrated photonic devices, such as optical filters,[1,2] optical modulators/switches,[3,4] and ring lasers.[5] Microring resonators with a high quality factor can even be employed to explore nonlinear effects,[6,7] low-threshold lasers,[5] and high speed optical modulators.[8,9] Silicon-on-insulator (SOI) is a promising material for an integrated photonic system, because of low cost and high index contrast, as well as compatibility with silicon microelectronics and fabrication facility. Niehusmann *et al*[10] have reported on an ultra-high quality factor microring resonator, based on SOI strip waveguides and TM-polarized mode operating. Moreover, rib waveguide racetrack resonators of high quality were also realized.[11] However, it is problematic to dope impurity and make metal contact in active devices for strip waveguide ring resonators. Then because of large dimensions and narrow free spectrum range, those resonators in Ref.[11] are not promising candidates for high-density optical communication systems. Therefore, we present a rib waveguide microring resonator with high performance and small dimension, achieving a compromise between compactness and functional extension.

In this work, we report on the detailed design and the realization of a high-performance microring resonator in an SOI rib waveguide, with a quality factor of 21200 and an extinction ratio of 12.5dB. From the measured results, we also determine the propagation loss in the curved waveguide to be only 0.89dB/mm. To minimize the propagation loss, by improving the relevant processes, including electron beam lithography (EBL) and inductively coupled plasma (ICP) etching, resonators with even a higher quality factor can be obtained.

2. Design

It is known that the quality factor and extinction ratio are two main parameters to characterize resonators. From the transfer functions of ring res-

*Project supported by the State Key Development Program for Basic Research of China (Grant Nos 2006CB302803 and 2007CB613405), the National High Technology Research and Development Program of China (Grant No 2006AA03Z424) and the National Natural Science Foundation of China (Grant No 60577044).
†E-mail: jzyu@red.semi.ac.cn

onators given by Yariv,[12] expressions of quality (Q) factor and extinction ratio (ER) can be deduced, respectively, as follows:

$$Q = \frac{\pi L N_{\text{eff}}}{\lambda_0} \frac{[\alpha(1-k)]^{1/4}}{1-\sqrt{\alpha(1-k)}}, \quad (1)$$

$$\text{ER} = \left[\left(\frac{\sqrt{1-k}-\sqrt{\alpha}}{\sqrt{1-k}+\sqrt{\alpha}} \right) \left(\frac{1+\sqrt{\alpha(1-k)}}{1-\sqrt{\alpha(1-k)}} \right) \right]^2, \quad (2)$$

where α is the power round-trip loss in the ring and k is the power coupling efficiency between the bus and the adjacent bent waveguide in a coupling region. The resonator perimeter, effective refractive index of the mode propagating in the ring, and resonant wavelength are denoted as L, N_{eff}, and λ_0, respectively. That is to say, coupling efficiency and round-trip loss are two main factors to influence the quality factor and the extinction ratio. We present their relations in Fig.1 at a resonant wavelength of 1550nm, with an N_{eff} of 2.8 and a ring radius of 40μm. It is evident that the quality factor decreases with the increase of coupling efficiency or round-trip loss (it is lossless for α=1). On the other hand, the extinction ratio depends on the relation between those two factors, and reaches a maximum at critical coupling ($k+\alpha$=1).

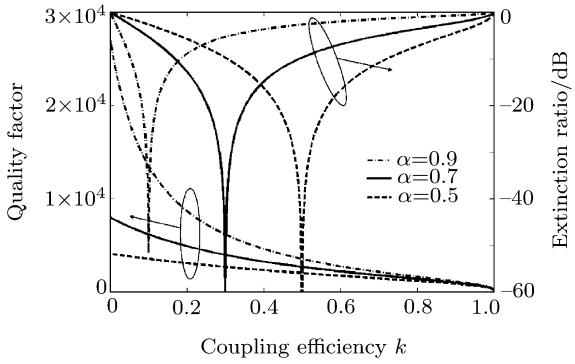


Fig.1. The quality factors and the extinction ratios each as a function of coupling efficiency for different round-trip losses.

Compared with the rib structure commonly used for large cross-section waveguides, the rectangular structure is more favourable when dimensions are scaled down to submicrometre level. However, submicrometre rib waveguides are still valuable for their mode characteristics, low propagation loss, and functional flexibility. Here, we choose a rib structure with a rib height (H) of 340nm, a slab height (h) of 170nm, and a rib width (W) of 420nm (see Fig.3(a)). Simulation results show that only a mode i.e. fundamental TE-polarized mode exists in this waveguide. Note that for rib waveguides with small dimensions, the traditional single mode condition no longer holds true, which is also stated by Lim *et al.*[13]

Bending loss, affected by the waveguide structure and bending radius, plays an important role in the round-trip loss. We simulate the bending loss by using the method presented by Subramaniam *et al.*[14] First, reduce a three-dimensional rib waveguide to a two-dimensional (2D) slab waveguide by using the effective index method. Then, calculate the bending loss by using a 2D analysis based on Marcuse's equation for that bending slab waveguide. The bending losses of a 90° bend as a function of bending radius are shown in Fig.2(a) for the cases in which the rib height is 340nm, the slab height is 170nm, and the rib widths are 350, 400, 450, 500nm. We observe that the bending loss decreases with the increase of bending radius exponentially, and it is negligible for radius $\geq$40μm with the rib widths being 350, 400, 450 and 500nm. As shown in Fig.2(b), the coupling efficiency is also simulated by using commercially available software FIMMPROP. Obviously, the coupling efficiency decreases monotonically for gap > 0.25μm, while peaks appear for the gaps ranging from 0.1μm to 0.25μm, and these peaks are attributed to the light coupling back from the bent waveguide. It is also seen

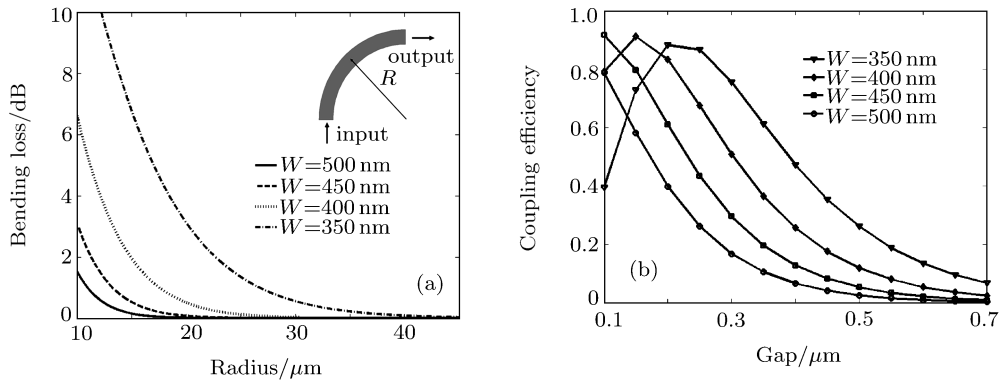


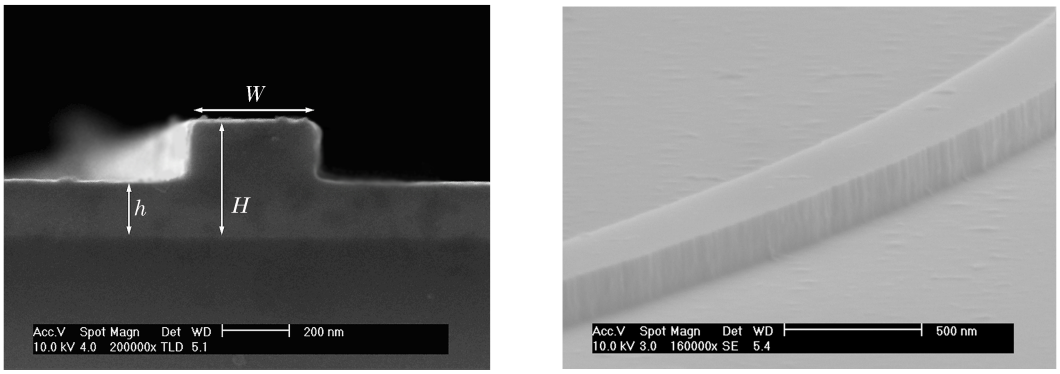
Fig.2. (a) The bending loss as a function of ring radius, (b) the coupling efficiency as a function of gap between ring and adjacent bus, with bending radius R=40μm, H=340nm, and h=170nm.

that both the bending loss and the coupling efficiency decrease with the increase of rib width, which is due to the strict optical confinement and low coupling coefficient for wide waveguides.

3. Fabrication

As stated above, low propagation loss, including bending loss and scattering loss, is of great significance for ring resonators. Scaling down the waveguide size and the deep etching for rib waveguides are two main methods to reduce bending loss. However, scattering loss becomes more sensitive to sidewall roughness while reducing the waveguide dimensions, since the optical field more extends to the waveguide boundaries. Therefore, in experiment, EBL and ICP etching were adopted to realize small size waveguides, and appropriate process parameters were exploited to reduce the sidewall roughness.

The sample was fabricated on a unibond-type SOI wafer with a 340nm-thick top silicon layer and 1μm-thick buried silica layer. EBL (Raith150) and ICP processes were used to fabricate the submicron waveguides[15] and microring resonator. First, a 195nm-thick polymethylmethacrylate (PMMA) 950K e-beam resist layer was spun-coated on the top silicon layer from a 4% solution in ethyl lactate. Next, the PMMA layer was pre-baked for 10 min at 180° to harden the resist. We optimized the electron dose and the expose step size to make proximity effect weak and pattern edge smooth. The exposed PMMA was developed in a methyl isobutyl keton (MIBK): iso-propyl alcohol (IPA)=1:3 solution and then rinsed in IPA, both for 18s. Following that, the ICP etching of the sample was performed by using the Alcatel-601E system. Remaining PMMA was removed subsequently. Finally, the sample was cleaved and the facet was polished for scanning electron microscopy (SEM) and measurement of optical characteristics.



(a) (b)

Fig.3. SEM images of cross section of the submicron rib waveguide (a) and side view of a curved waveguide based on silicon-on-insulator (b).

After that, submicron rib waveguides based on the SOI were realized. A cross section view and a side view of a bent waveguide are shown in Figs.3(a) and 3(b), respectively. The top cladding of the waveguide core is air, thus the high index contrast provides a strong optical confinement. The measured rib height (H), rib width (W), and slab height (h) are 340nm, 420nm, and 170nm, respectively, supporting only a fundamental TE-polarized mode. Figure 4 shows the SEM images of the microring resonator, including a close-up of coupling region in the inset. The ring radius and the gap between the ring and adjacent bus were measured to be 40μm and 440nm, respectively. Thus, the scattering loss, instead of bending loss (see

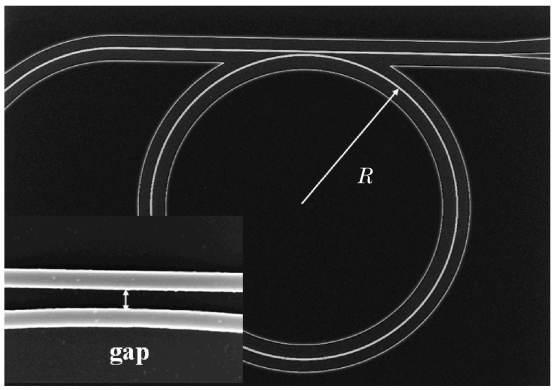


Fig.4. Scanning electron microscopy of the microring resonator with a radius of 40μm, and the inset shows close-up of the coupling region with gap=440nm.

Fig.2(a)), is the main loss mechanism in the ring resonator.

4. Measurement and results

The device was characterized by coupling light from a broad-band light emitting diode, which supplied a nearly uniform power at wavelengths ranging from 1540 to 1560nm, through a lensed fibre into the waveguide. A taper configuration from the sample facet to waveguide was used to increase the coupling efficiency between the single mode fibre and waveguide. The output light was collimated by a microscopy objective, and then collected by an infrared camera. By observing the spot, we tuned the position of input fibre and device under test. When the input fibre was rightly coupled, then the objective was removed and another lensed fibre was placed near the facet of output waveguide, and the end of fibre was connected to a power meter. The position of output lensed fibre was adjusted for an exact coupling, according to the display of power meter. Finally, the power meter was replaced by an optical spectrum analyser, and the transmission spectrum of ring resonator was ready to be measured.

Normalized with a spectrum for an independent bus waveguide, the transmission spectrum of ring resonator has been obtained at wavelengths ranging from 1548.6 to 1550nm as shown in Fig.5. Resonance of the ring has been observed at a wavelength (λ_0) of 1549.32nm, and the superposed oscillation is due to Fabry–Perot cavity effect, which results from the polished input/output facets and light reflecting. The extinction ratio and the bandwidth ($\Delta\lambda_{\mathrm{FWHM}}$) at a resonant wavelength were measured to be 12.5dB and 0.073nm, respectively, corresponding to a quality factor ($\lambda_0/\Delta\lambda_{\mathrm{FWHM}}$) as high as 21200. We also measured the optical spot at output port with an infrared camera and demonstrated the oscillation of resonator, by using a tunable DFB laser as a light source instead of a light emitting diode. As shown in Fig.5, the spot at output port is large and bright at non-resonant wavelengths such as 1548.80nm, while it is small and weak at a resonant wavelength (λ_0) of 1549.32nm.

In this waveguide, the N_{eff} of fundamental TE-polarized mode is 2.8110, derived from the resonant wavelength. Applying expressions (1) and (2) to fitting the experimental results, we obtain a coupling efficiency of 0.0801 and a round-trip loss of 0.9498, indicating that the critical coupling is almost achieved. As the round-trip loss and ring radius are 0.2238dB and 40μm, respectively, a low propagation loss of 0.89dB/mm in the curved waveguide is also demonstrated. To further improve the EBL and ICP processes, or use thermal oxidation, the sidewalls of waveguides should be smoothed and the propagation loss should be reduced as well.

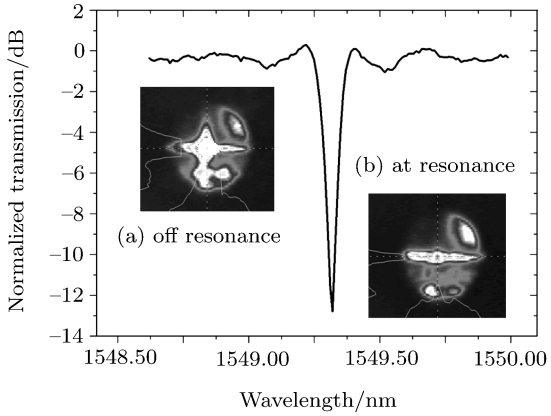


Fig.5. Measured transmission spectrum for the microring resonator, with an inset showing output spot at a non-resonant wavelength (a) and output spot at the resonant wavelength (b).

5. Conclusion

A high-performance microring resonator in an SOI rib waveguide has been designed and realized, with a quality factor of 21200, and an extinction ratio of 12.5dB. Propagation loss in the ring is minimized, and coupling efficiency is appropriately chosen for critical coupling. In the experiment, submicron rib waveguides are fabricated by EBL and ICP etching, and a low propagation loss of 0.89dB/mm is demonstrated in a curved waveguide. To further minimize the propagation loss, by optimizing the process parameters, even a higher quality factor could be achieved. In the future, electric structure will be added to make active devices, such as high speed optical modulators.

Acknowledgments

The authors thank Hejun Yu, Xiaoguang Tu, Xu Zhang and Hongjie Wang for valuable discussions, and great help in experiment.

References

[1] Little B E, Foresi JS, Steinmeyer G, Thoen E R, Chu S T, Haus H A, Ippen E P, Kimerling L C and Greene W 1998 *IEEE Photon. Technol. Lett.* **10** 549

[2] Little B E, Chu S T, Absil P P, Hryniewicz J V, Johnson F G, Seiferth E, Gill D, Van V, King O and Trakalo M 2004 *IEEE Photon. Technol. Lett.* **16** 2263

[3] Guarino A, Poberaj G, Rezzonico D, Degl'Innocenti R and Gunter P 2007 *Nature Photonics* **1** 407

[4] Nawrocka M S, Liu T, Wang X and Panepucci R R 2006 *Appl. Phys. Lett.* **89** 071110

[5] Rong H S, Kuo Y H, Xu S B, Liu A S, Jones R and Paniccia M 2006 *Opt. Express* **14** 6705

[6] Ibrahim T A, Grover R, Kuo L C, Kanakaraju S, Calhoun L C and Ho P T 2003 *IEEE Photon. Technol. Lett.* **15** 1422

[7] Zhao Y and Huo Y P 1987 *Acta Phys. Sin.* **36** 909 (in Chinese)

[8] Xu Q F, Manipatruni S, Schmidt B, Shakya J and Lipson M 2007 *Opt. Express* **15** 430

[9] Li J Q, Bananej A, Li Q H, Chen Q and Li C F 2004 *Chin. Phys.* **13** 1046

[10] Niehusmann J, Vorckel A, Bolivar P H, Wahbink T, Henschel W and Kurz H 2004 *Opt. Lett.* **29** 2861

[11] Kiyat I, Aydinli A and Dagli N 2005 *Opt. Express* **13** 1900

[12] Yariv A 2000 *Electron. Lett.* **36** 321

[13] Lim S, Png C E, Ong E A and Ang Y L 2007 *Opt. Express* **15** 11061

[14] Subramaniam V, De Brabander G N, Naghski D H and Boyd J T 1997 *J. Lightwave Technol.* **15** 990

[15] Tang H X, Zuo Y H, Yu J Z and Wang Q M 2007 *Chin. Phys.* **16** 2011